Neutron scattering study of single crystals of NpAs and NpSb



1991 J. Phys.: Condens. Matter 3 3551

(http://iopscience.iop.org/0953-8984/3/20/016)

J. Phys.: Condens. Matter 3 (1991) 3551–3562. Printed in the UK

# Neutron scattering study of single crystals of NpAs and NpSb

D L Jones†, W G Stirling†, G H Lander‡, J Rebizant‡, J C Spirlet‡, M Alba§ and O Vogt‖

† School of Physical Science and Engineering, Department of Physics, Keele University, Keele, Staffordshire ST5 5BG, UK

‡ Commission of the European Communities, Institute for Transuranium Elements, Joint Research Centre, Postfach 2340, D-7500 Karlsruhe, Federal Republic of Germany

§ Institut Laue–Langevin, BP 15X, 38042 Grenoble, France

‖ Laboratorium für Festkörperphysik, Eidgenössische Technische Hochschule, CH-8093 Zürich, Switzerland

Received 6 December 1990

**Abstract.** Neutron scattering experiments have been performed on single crystals of NpAs and NpSb. We report the critical exponents and a detailed investigation of the complex magnetic phase diagram of NpAs as a function of temperature. The anisotropy ratios in the critical scattering are 2.9(5) and 4.5(10) in NpAs and NpSb, respectively. The incommensurate-to-commensurate transition in NpAs is studied and found to be consistent with the McMillan approach, which is based on a Landau expansion. The 4+, 4− magnetic structure that exists over a narrow temperature range in NpAs is almost a complete square-wave modulation. These results, taken together with those for the isostructural uranium monopnictides, indicate the importance of invoking anisotropic interactions. Our experiments provide strong motivation for extending the theories to Np, the element following uranium, and in the trivalent state having the configuration $5f^4$.

## 1. Introduction

The magnetic properties of the uranium monopnictides (UN, UP, UAs, and USb), which all have the FCC NaCl crystal structure, have been examined extensively by neutron and other techniques over the last two decades (Rossat-Mignod *et al* 1984). Perhaps the most important new physics to emerge from these studies has been that the materials cannot be treated as localized 5f electron systems in which the ground-state wave function is determined primarily by crystal-field theory. Although this localized f-electron picture works well for the isostructural rare-earth (4f) compounds, the greater spatial extent of the 5f as compared to that of the 4f electrons has the consequence that the conventional crystal-field interactions are not the dominant ones. Instead theoretical efforts (Cooper *et al* 1985, Wills and Cooper 1987) have shown that the 5f electrons hybridize strongly with the conduction electrons, as well as possibly with other electron states (Sinha *et al* 1980). A key feature of this hybridization is that it is anisotropic, and the result is that the magnetic properties of these compounds are also highly anisotropic.

As we progress across the actinide (5f) series we anticipate that the 5f electrons will become more localized and that the properties will resemble those found in the analogous

rare-earth (4f) compounds. It is this aspect of the research, together with the unusual properties discovered, that motivates efforts on transuranium materials, despite the obvious difficulties of working with such materials.

In this paper we report detailed neutron investigations of single crystals of NpAs and NpSb. The first landmark study of these materials in polycrystalline form was reported by Aldred *et al* (1974) from Argonne National Laboratory. The development of methods to grow single crystals has meant that important new details can be discovered. Experiments have also been reported more recently on single crystals of NpAs (Burlet *et al* 1987a) and NpSb (Burlet *et al* 1988). These latter neutron experiments have determined the magnetic phase diagram as a function of applied magnetic field.

## 2. Experimental details

The preparation and growth of these transuranium single crystals is performed at the European Institute for Transuranium Elements, Karlsruhe. Full details are given by Spirlet and Vogt (1984) and Vogt and Spirlet (1987). Briefly, compressed pellets of the materials are kept in vacuum in tungsten crucibles for long periods (~10 days) at temperatures some 20 to 50 °C below their melting points. For NpAs and NpSb these are 2200 °C and 2000 °C, respectively. The most common isotope $^{237}$Np has been used. The absorption of $^{237}$Np at thermal neutron energies (25 meV) is quite large, 180 b, and this reduces the intensity of scattered neutrons. The samples were oriented and encapsulated at Karlsruhe in special Al double-walled containers approved by the Institut Laue–Langevin, Grenoble, France for neutron experiments. A specially adapted 'orange' cryostat is used at the ILL that has the facility to monitor the pressure around the container and detect the presence of any alpha emitters, which would indicate a breach in the containers.

The crystal of NpAs was a rectangular parallelepiped of dimensions $3.1 \times 2.8 \times 2.3\ \text{mm}^3$ with a mass of 0.174 g. It was oriented with the [110] axis vertical and axes [001] and [110] in the scattering plane, as is shown in figure 1. The NpAs crystal was of excellent quality and because of the interesting phase diagram of NpAs extensive neutron experiments were performed, and are described in section 3. The crystal of NpSb was much larger than the NpAs, with dimensions $\simeq 300\ \text{mm}^3$ and mass 2.9 g, having been originally prepared for inelastic neutron experiments. The crystal quality was poor and rocking curves showed that it was actually composed of a number of crystals. High-resolution diffraction experiments are difficult under these conditions and the investigation of NpSb is not as thorough as that of NpAs, but as the phase diagram of NpSb is much simpler than that of NpAs, this is not a serious concern.

The experiments have been performed on the IN 8 (with NpSb) and IN 14 (with both materials) triple-axis spectrometers at the Institut Laue–Langevin, Grenoble, France. The IN8 spectrometer is on a thermal source ($E_0$, the incident neutron energy being varied from $\simeq 10$ to $\simeq 80$ meV) and was used initially to search for inelastic magnetic excitations in NpSb, as in experiments on USb (Lander and Stirling 1980) and PuSb (Lander *et al* 1986). Unfortunately, these experiments on NpSb have not yet produced convincing evidence of inelastic excitations. Whether this is due to the high neutron absorption, and subsequent lack of intensity, or some unusual physics is not yet clear. Further efforts will be made with NpSb and other Np compounds.

The high-resolution experiments on NpAs were performed with the IN14 triple-axis spectrometer on the new horizontal cold source at ILL with incident energies from 5 to

20 meV. A fixed neutron energy of 5 meV was obtained from a vertically focused PG (002) monochromator. Collimation of 30′–40′–40′–40′ was employed, together with a Be filter to suppress second-order contamination. A matching PG analyser was used for most measurements, to reduce the background.

## 3. Experimental results on NpAs

### *3.1. General magnetic phase diagram*

The general magnetic phase diagram of NpAs as determined in this work is presented in figure 2. It is in good agreement with the earlier work of Aldred *et al* (1974) and Burlet *et al* (1987a), but is more detailed.

NpAs orders antiferromagnetically at $T_N = 173.6$ K with an incommensurate structure with a modulation vector of 0.233(1) reciprocal lattice units (RLU). The complete wave vector is written as $[0,0,q]$ because it corresponds to a longitudinal wave with the spin direction parallel to the propagation vector. By applying a magnetic field Burlet *et al* (1987a) have shown that this is a so-called single-$k$ structure (Rossat-Mignod *et al* 1984). This may be visualized as (001)-type sheets of Np spins stacked along the [001] direction with the magnitude of the magnetic moment following a sinusoidal modulation with a repeat distance od $1/q = 4.29(2)$ unit cells. In the single-$k$ structure there are three possible domains with modulations given by $[q,0,0]$, $[0,q,0]$ and $[0,0,q]$. These exist in different parts of the crystal; thus the magnetic symmetry in a single domain is tetragonal. The transition at $T_N$ is of second order. On further cooling, the intensity increases and the $q$-vector changes, moving towards the commensurate value of $q = \frac{1}{4}$ RLU. At $\simeq 168$ K a third harmonic (i.e. satellite peak appearing at the position $3q$) starts to appear.

At $T_{IC} = 158.2$ K NpAs becomes commensurate with $q = 0.25$ RLU. At the same time the third-order harmonic grows rapidly in magnitude and the magnetic structure in this region then corresponds closely to a 4+,4−,4+,4− modulation. Burlet *et al* (1987a) show that it remains a single-$k$ structure in this temperature range.

At $T_0 \sim 140$ K a *first-order* transition occurs from the $q = \frac{1}{4}$ to a $q = 1$ (type I) magnetic structure. There is considerable hysteresis ($\simeq 5$ K) associated with this transition and evidence for coexistence of the two phases. However, the latter effect is almost certainly a consequence of small thermal differences across the sample. Two other dramatic effects occur at this temperature. Aldred *et al* (1974) showed that the lattice symmetry changes from cubic above $T_N$ to tetragonal in the high temperature $q \leqslant 0.25$ RLU phases, but reverts to cubic on cooling through $T_0$. We emphasize that this is a most unusual transition, but can be understood by the measurements of Burlet *et al* (1987a) in which they show that NpAs becomes a triple-$k$ structure below $T_0$. In the triple-$k$ structure all three modulation wavevectors exist *simultaneously* within any given volume of the crystal. The symmetry of this magnetic structure is cubic and the moments point along the ⟨111⟩ directions. Hence the transitions cubic to tetragonal to cubic as NpAs passes through the phases paramagnetic to single $k$ ($q = \frac{1}{4}$), to triple $k$ ($q = 1$) with decreasing temperature. The other dramatic effect at $T_0$ is that the resistivity increases by several orders of magnitude (Aldred *et al* 1974, Fournier 1990), so NpAs changes at

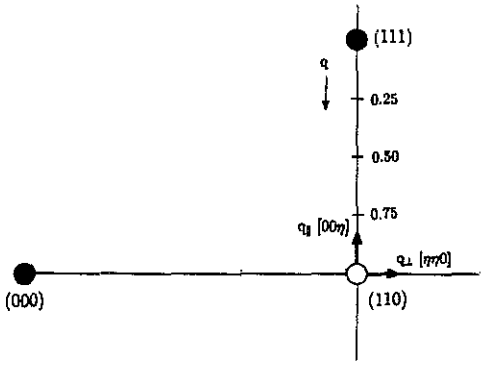


**Figure 1.** Schematic representation of reciprocal space examined in present experiments on NpAs and NpSb. The [1 −1 0] direction is vertical. The ordering wave vectors are along the line from (111) to (110) and are defined by the vector $q = (0,0,q)$ from (111). Brillouin zone centres are marked as full circles, zone boundaries as open circles.

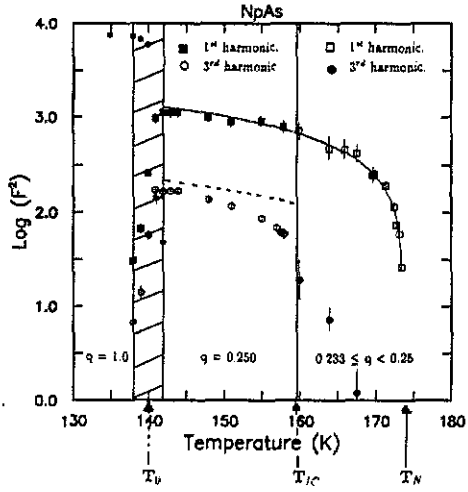


**Figure 2.** Details of the magnetic phase diagram in NpAs for $T > 130$ K. □, ●, intensities of first and third harmonics in the incommensurate phase for $T_{IC} < T < T_N$. ■, ○, intensities of first and third harmonics in the commensurate phase to $T_0 < T < T_{IC}$. The full curve is the least-squares fit to the $\beta$-parameter discussed in the text. The broken curve in the commensurate phase corresponds to the intensity predicted for a square-wave modulation. *, intensity of (110) peak in type-I phase for $T < T_0$.

$T_0$ from being a semimetal at high temperature to become a semiconductor at low temperature.

### *3.2. The critical regime near $T_N$*

As discussed in the Introduction an important feature of the magnetic interactions in the actinide monopnictides is that they are highly anisotropic. In forming the magnetic structures, in which (001) planes of actinide moments are stacked in various sequences along the [001] direction, the interactions *within* an (001) plane have been found to be much stronger than interactions *between* such planes. This can best be seen by measuring the magnetic correlations just above $T_N$. These correlations are anisotropic in the sense that the longer-range (and therefore stronger) correlations can be distinguished by measuring the directional dependence of the diffuse scattering above $T_N$ (Sinha *et al* 1980, Rossat-Mignod *et al* 1984). With reference to figure 1, by measuring the profile of the diffuse scattering at a point such as (110) in figure 1 in the [$\eta\eta$0] and [00$\eta$] directions we can immediately deduce the spatial extent of the correlations in these two directions, which correspond, respectively, to correlations within and between (001) planes of similar Np moments.

Figure 3 shows scans around the point $q = [0,0,0.233]$ in the [$\eta\eta$0] and [00$\eta$] directions at $T = 176.85$ K, which corresponds to a reduced temperature, $t = (T - T_N)/T_N$, of $1.85 \times 10^{-2}$. The inverse correlation length in the [00$\eta$] direction is $\kappa_{\parallel}$, where the

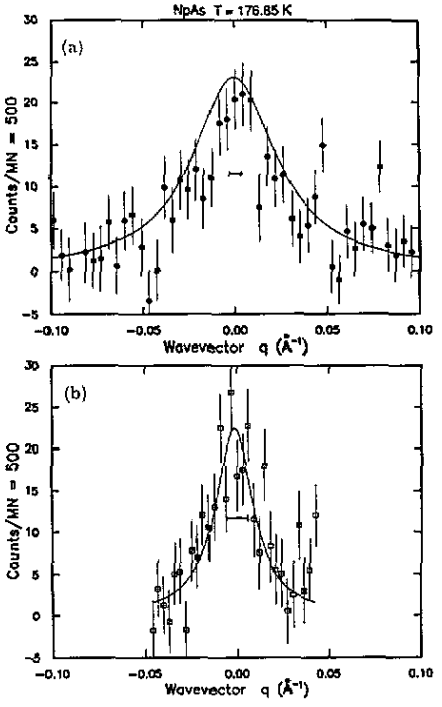


**Figure 3.** Experimental data from NpAs at 176.85 K, which correspond to $t = 1.85 \times 10^{-2}$, as measured near the point $\boldsymbol{q} = (0, 0, 0.233)$. (a) Direction $(00\eta)$. (b) Direction $(\eta\eta 0)$. The resolution function is shown as a vertical bar in each figure and the fits are indicated by full curves. All data on this and subsequent figures are normalized to a monitor of 500 ($\simeq$40 s), although most scans were taken with counting times four to eight times as long.

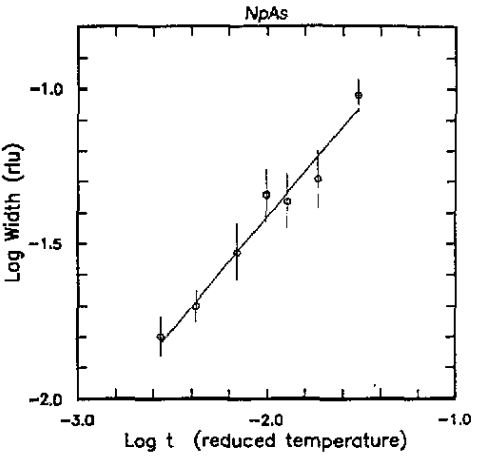


**Figure 4.** Inverse correlation lengths $\kappa_\parallel$ for NpAs as a function of reduced temperature. The least-squares fit gives $\nu = 0.73(2)$.

parallel sign is to indicate that the correlations are parallel to the direction of wavevector propagation. The real space correlation length $\xi$ is related to $\kappa_\parallel$ by $\kappa_\parallel = 2\pi/\xi_\parallel$, and a similar definition pertains to $\zeta_\perp$ and $\kappa_\perp$. The $\kappa$-values are deduced by fitting Lorentzians (suitably convoluted with the experimental resolution function, taken to be a Gaussian) to data taken in the $[\eta\eta 0]$ and $[00\eta]$ directions. A convenient measure of the anisotropy (Burlet *et al* 1987b) is then

$$R = \kappa_\parallel/\kappa_\perp. \tag{1}$$

The instrumental resolution in the $[\eta\eta 0]$ direction is such that measurements of the $\kappa_\perp$ are more difficult than those of $\kappa_\parallel$. From the data of figure 3 we determine $R = 2.9 \pm 0.5$ for NpAs. A fuller discussion of this $R$-value may be found in section 5.

As the material is cooled towards $T_N$ the real-space correlation lengths increase, and so both $\kappa_\parallel$ and $\kappa_\perp$ decrease. Since $\kappa_\perp$ is small at all times it is difficult to deduce its

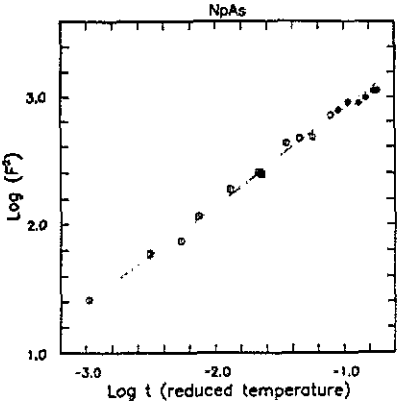


**Figure 5.** Integrated intensity ($F^2$) versus reduced temperature for the first harmonics of NpAs below $T_N$. The least-squares fit gives $\beta = 0.38(1)$ and $T_N = 173.64(5)$ K. Open (full) symbols correspond to Bragg peaks above (below) $T_{IC}$.

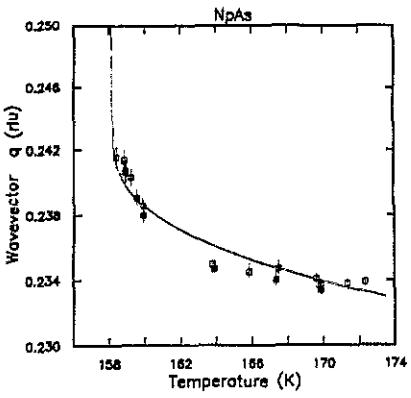


**Figure 6.** Variation of the modulation vector as a function of temperature in the incommensurate region. Open (full) symbols correspond to $q$ determined from first-order (third-order) peaks. The full curve represents a least-squares fit to the McMillan expression, equation (4).

behaviour accurately as a function of temperature. Figure 4 shows $\kappa_{\parallel}$ as a function of temperature. We anticipate that

$$\kappa = \kappa_0 t^{\nu} \tag{2}$$

where $t$ is the reduced temperature and $\nu$ is the critical exponent. From the least-squares fit of figure 4 we find $\nu = 0.73(2)$. The anisotropy parameters and critical exponents are tabulated and further discussed in section 5. Since earlier experimental studies, and theory, have shown that $R$ is independent of temperature, we have not addressed this point further (Lander *et al* 1978, Burlet *et al* 1987b).

### *3.3. Incommensurate phase*

Below $T_N$ the increasing magnitude of the ordered moment may be expressed as a power law by the equation

$$F^2 = F_0^2 t^{2\beta} \tag{3}$$

where $F^2$ is the integrated intensity of the Bragg peak, which is proportional to the square of the magnetic moment, and $\beta$ is the staggered magnetization exponent. The least-squares fit as shown in figure 5 gives $\beta = 0.38(1)$ and $T_N = 173.64(5)$ K. Note that this relationship holds not only in the incommensurate phase near $T_N$ (see figure 2) but also below $T_{IC}$ in the commensurate phase.

As discussed above, the initial ordering wavevector below $T_N = 173.6$ K is $\approx 0.233$ but this gradually increases until at $T_{IC} = 158.2$ K the system locks in to the commensurate wave vector of $q = 0.250$ RLU. A theoretical description of an incommensurate–commensurate phase transition has been given by McMillan (1976). Although his arguments were for structural modulations they are also applicable to magnetic modulations. The predictions are that the transition to the commensurate state is continuous, but it resembles a first-order transition in the rapidity with which the

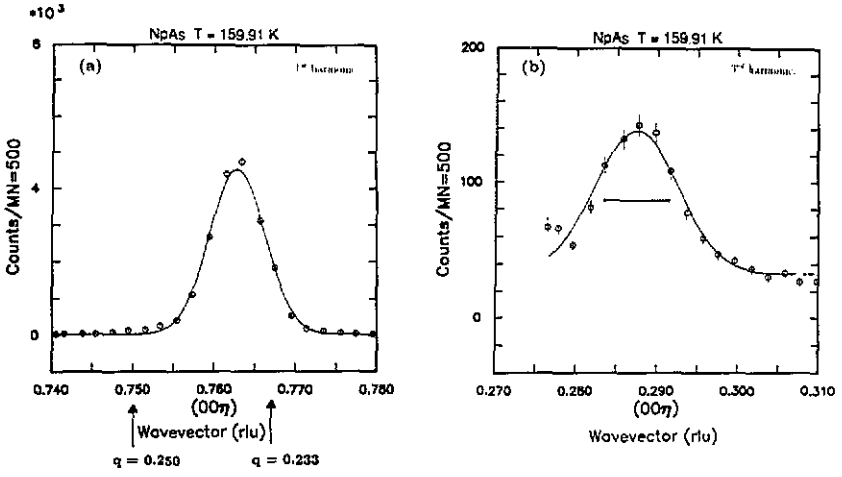


**Figure 7.** (*a*) Profile of the first-order harmonics satellite peak just above $T_{IC}$. (*b*) Profile of the third-order harmonic satellite peak just above $T_{IC}$. Note the resolution function marked with a bar. The third-order harmonic is ≈50% wider than the first harmonics at this temperature.

commensurate wavevector $q_{cm}$ is reached. We show in figure 6 the variation of the wave vector $q$ as a function of temperature. The full curve is the fit to the McMillan formula

$$q(t') = q_{cm} - (q_{cm} - q_{inc})\sigma(t') \tag{4}$$

where $\sigma(t') = 4.62/(4.61 + \ln(1/t'))$ and $t' = (T - T_{IC})/(T_N - T_{IC})$, with $T_{IC} = 158.2$ K, $T_N = 173.6$ K, $q_{cm} = 0.250$ and $q_{inc} = 0.233$. The fit in figure 6 shows that the data are consistent with the McMillan relationship.

That the transition at $T_{IC}$ is continuous may also be inferred from the smooth variation of the first-order harmonic as a function of temperature, as shown in figures 2 and 5. The first harmonic is always resolution limited (i.e. we cannot measure a finite correlation length, and so the magnetic modulation appears infinite in extent), but the third harmonic is notably wider than the resolution, as shown in figure 7. The appearance of the third-order harmonic implies a tendency for the waveform to resemble a square wave, but because of the incommensurate nature of the wave vector the waves can never be completely square. Formally, there can be no strict relationship between the phases of the first and third harmonics. Under these conditions it is reasonable to expect the weaker third-order harmonic to be spatially less well defined than the stronger first-order harmonic. By analysing the width in figure 7(b) the correlation length of the third-order harmonic at ≈160 K is ≈650 Å. However, at $T_{IC}$ the third-order intensity suddenly increases and the peak width becomes identical to the resolution function. This is because the third-order harmonic now contributes to the production of a perfect square wave.

### *3.4. Commensurate phase*

Below $T_{IC}$ (=158.2 K) the magnetic structure approaches the idealized 4+, 4−, 4+, 4− etc arrangement of magnetic moments. Aldred *et al* (1974) have discussed various possible arrangements of the moments (see table II of this reference) and it is clear from

this that the 4+, 4− arrangement is the only one consistent with our observation of only a first- and third-order harmonic. As is well known, diffraction experiments cannot determine the phase relationship between two modulations. We may write the moment values derived from the first- and third-order harmonics as

$$\mu_1^i = A_1 \sin(2\pi q z_i + \varphi_1) \qquad \mu_3^i = A_3 \sin(2\pi 3 q z_i + \varphi_3) \tag{5}$$

where $z_i$ specifies the relevant plane in the [001] direction (recall that all the moments in such a plane are identical), $A_1$ and $A_3$ are the wave amplitudes, and $\varphi_1$ and $\varphi_3$ are arbitrary phase angles.

By inspection it is simple to show that for the 4+, 4− configuration, i.e.

$$\mu = \mu_1^1 + \mu_3^1 = \mu_1^2 + \mu_3^2 = \mu_1^3 + \mu_3^3 = \mu_1^4 + \mu_3^4 = -(\mu_1^5 + \mu_3^5) = -(\mu_1^6 + \mu_3^6)$$
$$= -(\mu_1^7 + \mu_3^7) = -(\mu_1^8 + \mu_3^8)$$

and the phases are given by

$$\varphi_1 = \pi/8 \qquad \varphi_3 = 3\varphi_1. \tag{6}$$

For a perfect square wave the ratio $A_3/A_1$ is given by

$$A_3/A_1 = \frac{\sin\varphi_3 - \sin\varphi_1}{\sin\varphi_3 + \sin\varphi_1} = 0.4142 \tag{7}$$

and

$$\mu = A_1[\sin\pi/8 + (A_3/A_1)\sin 3\pi/8] = 0.7654\,A_1. \tag{8}$$

Since the intensity is proportional to the square of the amplitude, the ideal ratio of the structure factors $F_1$ and $F_3$, which are related to the intensities, $I$, by the geometric factor $F^2 = I\sin 2\theta$, where $\theta$ is the Bragg angle, is given by $(F_3/F_1)^2 = (A_3/A_1)^2 = 0.1716$ and this is marked with a broken curve in figure 2. We see that an almost perfect square wave is formed below $\simeq$150 K. So the sudden increase in the amplitude of $A_3$ near $T_{IC}$ is related to the phase locking of the first- and third-order harmonics and the decrease in entropy associated with the formation of a perfect square wave. It is interesting to note that such a perfect square wave is not observed in NpP (Aldred *et al* 1974, Lander *et al* 1973), in which the low-temperature wave vector is $q = \frac{1}{3}$. Finally, by comparing the magnitude of the magnetic peaks to that of the (111) nuclear reflection, the value of the ordered moment just above $T_0$ is $\sim 1\,\mu_B$.

### *3.5. Type-I structure*

At $T_0$ (142 K on cooling, 138 K on heating) a dramatic transition occurs in NpAs to the type-I magnetic structure, for which magnetic Bragg peaks occur at $q = 1$, i.e. (110) in figure 1. We have verified that this is a first-order transition as no critical scattering can be seen at $q = 1$ above $T_0$. In both heating and cooling cycles we observe peaks from both the $q = 0.25$ and $q = 1$ phases simultaneously present over a large (4 K) temperature range, but we believe this is a consequence of both natural hysteresis and thermal inhomogenities. The peaks are always resolution limited in this range.

Experiments with an applied magnetic field (Burlet *et al* 1987a) have shown that this low-temperature phase is a triple-$k$ structure, whereas for $T > T_0$ a single-$k$ structure is present. The symmetry of the triple-$k$ structure is cubic, and that of the single-$k$ structure is tetragonal (Rossat-Mignod *et al* 1984) which explains why NpAs is cubic below $T_0$,

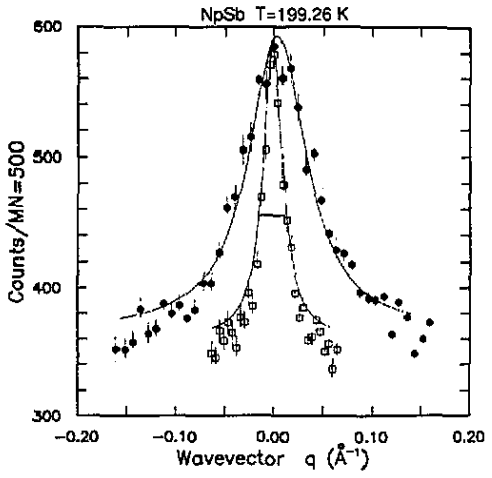


**Figure 8.** Similar scan to figure 3 for NpAs showing the anisotropy in the critical scattering at $T = 199.26$ K ($t = 1.3 \times 10^{-3}$) for NpSb. The symbols are the same as in figure 3.

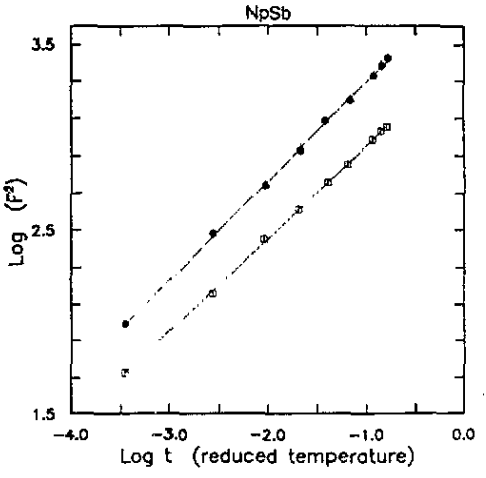


**Figure 9.** Integrated intensity ($F^2$) versus reduced temperature for the $q = 1$ Bragg peak in NpSb below $T_N$. Open squares (full circles) correspond to data taken with (without) an analyser. The least-squares fit give $\beta = 0.250(5)$ for the open squares and $\beta = 0.266(5)$ for the full circles. The value for $T_N = 199.01(2)$ K from the fit.

tetragonal for $T_0 < T < T_N$, and cubic again for $T > T_N$. Our resolution is insufficient to examine this aspect of the lattice symmetry. According to Aldred *et al* (1974) the largest extent of the tetragonal distortion at 143 K is $(c - a)/a = -8 \times 10^{-4}$. However, we do see a large increase in the intensity of the (111) and (200) nuclear reflections on heating through $T_0$ and this occurs because of the relief of extinction as the material distorts from cubic (below $T_0$) to tetragonal (above $T_0$). Below $T_0$ the extinction effects, which are greatly exaggerated because of our use of 4 Å (5 meV) neutrons, prohibit a precise determination of the magnetic moment, but they are consistent with earlier determinations (Aldred *et al* 1974, Burlet *et al* 1987a) of 2.5(1) $\mu_B$ at 4.2 K. Just below $T_0$ the moment is of the order of 2 $\mu_B$ so there is a substantial discontinuity in the value of $\mu$ at $T_0$.

## 4. Experimental results on NpSb

The magnetic phase diagram of NpSb is much simpler (Aldred *et al* 1974, Burlet *et al* 1988) than that of NpAs. At $T_N \simeq 200$ K NpSb adopts the $q = 1$ type-1 magnetic structure and experiments in an applied magnetic field show that this is a triple-$k$ ordering (Burlet *et al* 1988). At low temperature the ordered moment is 2.5(1) $\mu_B$.

Our experiments have been confined to measuring the critical exponent $\beta$, of (3), and to examining the anisotropy in the critical scattering just above $T_N$. Unfortunately, the rather poor quality of the crystal prevented a determination of the correlation exponent $\nu$, see (2). Figure 8, which should be compared to figure 3 for NpAs, shows directly the anisotropy in the critical scattering for NpSb. From a number of scans at different temperatures we deduce that the anisotropy ratio is 4.5 ± 1.0. The exponent

**Table 1.** Summary of critical parameters in Ce, U, Np and Pu monopnictides. $R$ is the anisotropy ratio (equation (1)). Numbers in parenthesis refer to standard deviations of the least significant digit.

| | Lattice parameter (Å) | $T_N$ (K) | $\beta$ | $\nu$ | $R$ | Reference |
|---|---|---|---|---|---|---|
| CeAs | 6.078 | 8 | — | — | 0.6(1) | a |
| CeSb | 6.412 | 16 | First-order transition | | 1.8(2) | b |
| CeBi | 6.487 | 25.4 | 0.317(5) | 0.63(6) | 2.5(2) | c |
| UN | 4.890 | ≈54 | 0.31(3) | 0.84(5) | 2.8(3) | d |
| UAs | 5.779 | 124 | First-order transition | | 3.8(5) | e |
| USb | 6.191 | 212.2 | 0.32(2) | 0.68(4) | 5.0(5) | f |
| NpAs | 5.838 | 173.6 | 0.38(1) | 0.73(2) | 2.9(5) | |
| NpSb | 6.254 | 199.0 | 0.257(5) | — | 4.5(10) | |
| NpBi | 6.438 | 192.5 | 0.31(2) | | | g |
| PuSb | 6.225 | 85.3 | 0.31(2) | 0.58(5) | 1.8(3) | h |
| Classical mean field | | | 0.5 | 0.5 | | |
| 3D Heisenberg | | | 0.345 | ≈0.7 | | |
| 3D Ising | | | 0.3125 | 0.64 | | |
| 2D Ising | | | 0.125 | 1.0 | | |

[a] Halg and Furrer (1986).
[b] Halg *et al* (1981).
[c] Halg *et al* (1982).
[d] Holden *et al* (1982).
[e] Sinha *et al* (1980).
[f] Lander *et al* (1978), Hagen *et al* (1988).
[g] Bourdarot and Burlet (1990).
[h] Burlet *et al* (1987b).

$\beta$ below $T_N$ for NpSb is determined for the intensity of the (1,1,0) peak as shown in figure 9. The fact that $\beta$ for both the two-axis and three-axis experiments are almost identical implies that the energy width of the critical fluctuations is very small. This was verified directly by making energy scans; a similar situation was found in USb, which also has the triple-$k$ structure (Lander *et al* 1978, Hagen *et al* 1988). The mean value of $\beta = 0.257(5)$.

## 5. Discussion

The critical exponents for the monopnictides of Ce, U, Np and Pu known to date are gathered in table 1. Because of the strong intraplane correlations, earlier discussions (Burlet *et al* (1987b) and references therein) suggested that the systems could be classed as 3D Ising systems. The anisotropic interactions strongly suggest such an interpretation, but the precise values of $\beta$ and $\nu$ must be obtained from a detailed description of the competing interactions within the framework of the ANNI model (Kaski and Selke 1985). It is interesting that NpSb and NpAs have, respectively, the lowest and highest values of $\beta$ so far determined. In most cases $\nu \simeq 2\beta$, which is the general expectation of 3D systems (the determintion of $\nu$ in UN is suspect because of the difficulty in determining $T_N$; see Holden *et al* 1982). Hopefully, as we complete the listing of these $\beta$- and $\nu$-values it will provide a motivation for exact calculations within the ANNI model.

The anisotropy ratio $R$ (see (1)) has been considered for Ce and Pu systems by Kioussis and Cooper (1986a, b), Hu *et al* (1987), and Cooper *et al* (1987). The $R$-values for these systems do not exceed 3, and they obtain reasonable agreement with

experiment. We should emphasize that the introduction of anisotropic interactions is central to the theories of Cooper *et al* (1985), so the first-principles calculation of these $R$-values represents an important test for these calculations. As noted by Burlet *et al* (1987b), the $R$-value was largest for USb, the only triple-$k$ system examined up to that time. NpSb, also a triple-$k$ system, has an $R$-value similar to that in USb. This suggests that these strong interactions, which give rise to a high ordering temperature, are also important in stabilizing the triple-$k$ structure, and have been discussed (Sinha *et al* 1980, Burlet *et al* 1988) in terms of direct mixing between the 5f electrons and the anion p band. Direct evidence for such mixing can be found in Mössbauer experiments at the Sb site in USb and NpSb (Sanchez *et al* 1987, 1990).

The phase diagram has been studied in some detail in NpAs. Entropy considerations lead to the initial incommensurate ordering wave vector becoming commensurate (the requirement at low temperature to have all the moments the same magnitude) and result in an almost 4+,4− configuration. The wave vector dependence closely follows the predictions of McMillan (1976). However, the transition at $T_0$ is certainly electronic in origin and the type-I triple-$k$ structure is formed with an enormous increase in resistivity (Aldred *et al* 1974, Fournier 1990), and a large jump from about 1 to 2 $\mu_B$ in the ordered moment at each Np site. Further characterization of this transition is anticipated from Hall-effect measurements currently in progress by Fournier and collaborators.

In conclusion, our experiments show clearly that the Np monopnictides are equally as complex in their magnetic properties as their uranium analogues, Indeed NpAs is probably the most complex monopnictide investigated to date. Thus, although the localization increases for a heavier anion, the competing interactions can still lead to complex behaviour. It will be most interesting to compare planned (Cooper 1990) theoretical values for $R$ with those given in table 1.

## Acknowledgments

We are grateful to Paul Burlet and Jean Rossat-Mignod for letting us quote the unpublished $\beta$-value for NpBi in table 1, and also to them and Barry Cooper for useful discussions. We are grateful to the ILL for the provision of the neutron scattering facilities used in this work and thank the Radio-Protection Services for their cooperation in performing neutron experiments on transuranium samples. The assistance of Ces Rijkeboer in growing the crystals is appreciated. One of us (DLJ) thanks the Science and Engineering Research Council (UK) for the provision of a studentship.

## References

Aldred A T, Dunlap B D, Harvey A R, Lam D J, Lander G H and Mueller M H 1974 *Phys. Rev.* B **9** 3766

Bourdarot F and Burlet P 1990 private communication

Burlet P, Bonnisseau D, Quezel S, Rossat-Mignod J, Spirlet J C, Rebizant J and Vogt O 1987a *J. Magn. Magn. Mater.* **63–64** 151

Burlet P, Quezel S, Bonnisseau D, Rossat-Mignod J, Spirlet J C and Rebizant J 1988 *Solid State Commun.* **67** 999

Burlet P, Rossat-Mignod J, Lander G H, Spirlet J C, Rebizant J and Vogt O 1987b *Phys. Rev.* B **36** 5306

Cooper B R 1990 private communication

Cooper B R, Hu G J, Kioussis N and Wills J M 1987 *J. Magn. Magn. Mater.* **63–64** 121

Cooper B R, Sieman R, Yang D, Thayamballi P and Banerjea A 1985 *Handbook on the Physics and Chemistry of the Actinides* vol 2, ed A J Freeman and G H Lander (Amsterdam: North-Holland) pp 435–500

Fournier J M *et al* 1990 private communication
Hagen M, Stirling W G and Lander G H 1988 *Phys. Rev.* B **37** 1984
Halg B and Furrer A 1986 *Phys. Rev.* B **34** 6258
Halg B, Furrer A, Halg W and Vogt O 1981 *J. Phys. C: Solid State Phys.* **14** L961
—— 1982 *J. Magn. Magn. Mater.* **29** 151
Holden T M, Buyers W J L, Svensson E C and Lander G H 1982 *Phys. Rev.* B **26** 6227
Hu G J, Kioussis N, Cooper B R and Banerjea A 1987 *J. Appl. Phys.* **61** 3385
Kaski K and Selke W 1985 *Phys. Rev.* B **31** 3128 and references therein
Kioussis N and Cooper B R 1986a *Phys. Rev.* B **34** 3261
—— 1986b *J. Magn. Magn. Mater.* **54–57** 701
Lander G H, Dunlap B D, Mueller M H, Nowik I and Reddy J F 1973 *Int. J. Magn.* **4** 99
Lander G H, Sinha S K, Sparlin D M and Vogt O 1978 *Phys. Rev. Lett.* **40** 523
Lander G H and Stirling W G 1980 *Phys. Rev.* B **21** 436
Lander G H, Stirling W G, Rossat-Mignod J, Spirlet J C, Rebizant J and Vogt O 1986 *Physica* B **136** 409
McMillan W L 1976 *Phys. Rev.* B **14** 1496
Rossat-Mignod J, Lander G H and Burlet P 1984 *Handbook on the Physics and Chemistry of the Actinides* vol 1, ed A J Freeman and G H Lander (Amsterdam: North-Holland) pp 415–500
Sanchez J P, Spirlet J C, Rebizant J and Vogt O 1987 *J. Magn. Magn. Mater.* **63–64** 139
Sanchez J P, Tomala K, Rebizant J, Spirlet J C and Vogt O 1990 *Hyperfine Interac.* **54** 701
Sinha S K, Lander G H, Shapiro S M and Vogt O 1980 *Phys. Rev. Lett.* **45** 1028
—— 1981 *Phys. Rev.* B **23** 4556
Spirlet J C and Vogt O 1984 *Handbook on the Physics and Chemistry of the Actinides* vol 1, ed A J Freeman and G H Lander (Amsterdam: North-Holland) p 79
Vogt O and Spirlet J C 1987 *J. Magn. Magn. Mater.* **63–64** 683
Wills J M and Cooper B R 1987 *Phys. Rev.* B **36** 3809